dgements

ors would like to acknowledge the financial sponsorship of the
uded in this paper by several Australian Mining Companies,
or through the Australian Mineral Industries Research
td. Members staff of the companies have provided invaluable
in all projects.
ors would like to express their sincere thanks to all members
he Division with whom they have worked collaboratively on the
cts:

ed grouted steel dowels - Dr. P.G. Fuller, Mr. R.H.T. Cox.

tion of crown pillars - Mr. G. Worotnicki, Mr. A. Spathis.

pe investigation - Mr. L.G. Alexander, Mr. S. Mathews.

le and high-wall stability - Dr. P.G. Fuller, Mr. R.H.T. Cox.

es

by, D.R. - "Techniques Applicable in Mining Industry Investigations"
RO, Division of Applied Geomechanics, Technical Report, 1974.

A.H. - "A Laboratory Investigation of a High Modulus Borehole
g Gauge for the Measurement of Rock Stress" 4th Symposium on
k Mechanics, Pennsylvania State University, 1961.

ki, G. and Walton, R.J. - "Triaxial Hollow Inclusion Gauges for
ermination of Rock Stresses in-situ". Investigation of Stress
Rock, Advances in Stress Measurement, I.S.R.M. Conference,
ney, 1976.

ki, G., Enever, J.R. and Spathis, A. - "A Pressiometer for
erming Deformation Modulus at Rock in-situ". Symposium,
situ Testing for Design Parameters, Aust. Geomechanics
iety, Victoria Group, Melbourne, 1975.

ki, G., Alexander, L.G., Willoughby, D.R. and Ashcroft, J.F. -
formation and Behaviour of High Rise Filled Stopes at CSA Mine,
ar, N.S.W." Proc., 2nd Aust. - N.Z. Conf. on Geomechanics,
bane, 1975.

VIBRATION OF TUNNEL DUE TO ADJACENT BLASTING OPERATION

Shunsuke Sakurai[1] and Yasutoshi Kitamura[2]

1. Introduction

In recent years, the construction of utility tunnels has been quite active because of the effective use of land and the settlement of environmental problems. And the demand will increase more in the future. Under these circumstances, it is quite often necessary for a newly constructed tunnel to cross three-dimensionally with an existing old tunnel in the underground medium. When the construction works are conducted by blasting, much attention must be paid to the blasting operation in order not to cause any serious damage on the existing tunnel.

Dynamic behaviors of underground structures like tunnels due to blasting have not yet been clearly understood. Therefore, there are difficulties in establishing controlled blasting techniques. Determinations of charge weight, its pattern and design criterion for vibration of structure are based on previous experiences.

In order to establish controlled blasting techniques to avoid damage in an adjacent tunnel, the dynamic behavior of the tunnel under blast excitation must be first understood. For this purpose, some field works have been conducted. This paper is concerned with the results of these field experiments. This consists of two parts, the first is concerned with the dynamic behavior of two unlined tunnels which three-dimensionally cross each other in the underground medium, the second part is for the dynamic behavior of the concrete lining of tunnels due to an adjacent blast, and much attention is paid to discussing the relation between the particle velocity and the strain in the lining.

2. Dynamic Behaviors of Two Unlined Tunnels

2.1 Test Site

The test site where the experimental works have been conducted is shown in Fig. 1. There are two tunnels embedded in this site; one is designed as a water supply tunnel (called Tunnel A), and the other is for an underground subway (called Tunnel B). Both tunnels are under construction, so that no liners are installed as yet. The crossing angle of these two tunnels is about 78° in a level plane. The clearance between the two tunnels is 29.7m at the excavation of a pilot tunnel, which is located at the bottom of Tunnel B, and 24.5m at the excavation of the upper part of Tunnel B. The underground formation around the tunnels consists of granite, and the propagation velocity of the longitudinal wave is approximately 3.0 ~ 3.7km/s.

[1] Professor of Civil Engineering, Kobe University, Kobe, Japan
[2] Research Associate, Kobe University, Kobe, Japan

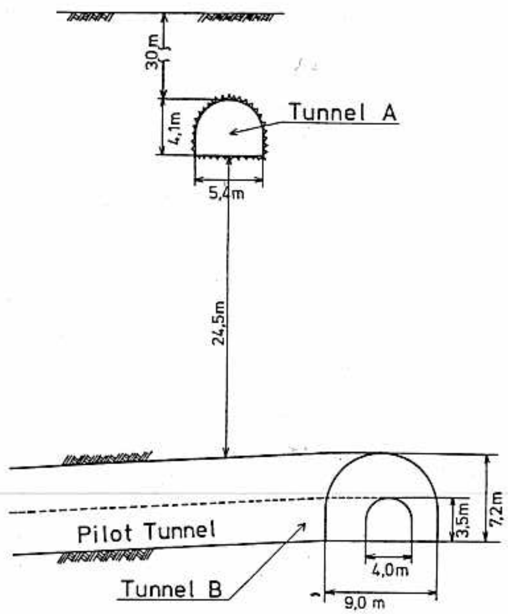

Fig. 1 Section View of Two Tunnels

2.2 Instrumentation

The particle velocities on the surface of the tunnels were measured by electromagnetic-type velocity gages (Geo-space: natural frequency $f_0 = 4.5$Hz and 8Hz). The data are recorded on an electromagnetic oscillograph through a direct current amplifier. The velocity gages were directly mounted on the bottom rock surface of both tunnel A and B with cement mortar. The blasting operation was done only at the face of tunnel B and all measurements were taken at the same time for each blast.

2.3 Results and Discussions

(1) Comparison of Particle Velocity in Tunnel A and Tunnel B

Particle velocities measured at Tunnel A are compared with those at Tunnel B, as shown in Fig. 2. These measurements have been obtained for blasting operations at three different positions of the face of Tunnel B, but the measuring points in both tunnels are located at the same distance from the blast zone. Time-delay shots are used for blasting. The results are plotted against each shot.

Fig. 2 (a) shows the ratio of the vertical component in Tunnel A against the horizontal component in the direction of the axis of Tunnel B, where the horizontal component usually gives the maximum value. On the other hand, Fig. 2 (b) shows the ratio of the vertical component in Tunnel A against the vertical in Tunnel B. It can be seen from Fig. 2 (b) that the magnitude of the particle velocity in Tunnel A may become more than ten times greater than in Tunnel B, and the vertical component of Tunnel A gives a $2 \sim 7$ times greater magnitude than the horizontal component, depending on the location of blast zone. The maximum value of this ratio is obtained when the face of the tunnel approaches to within 30m of the crossing point, and this ratio tends to decrease as the tunnel face approaches the crossing point and passes through it.

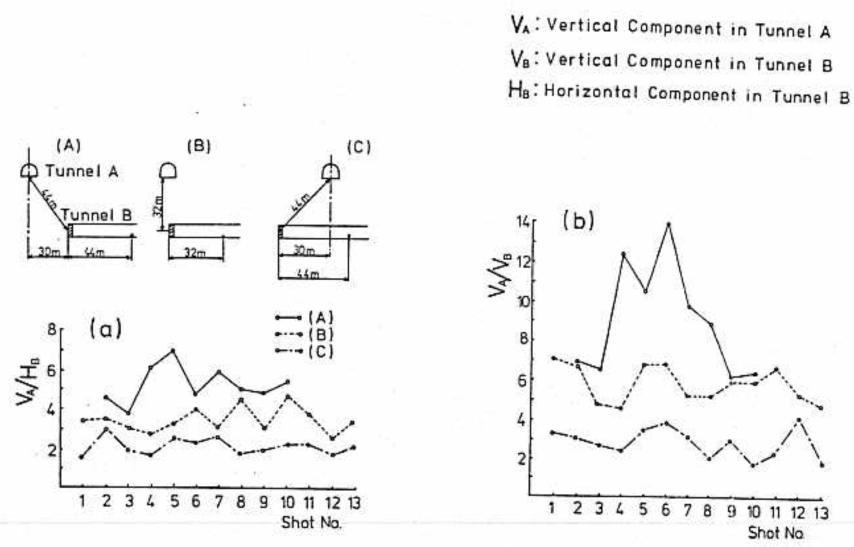

Fig. 2 Ratio of Particle Velocities

These results give valuable information as in the following case. When the face of the new tunnel approaches an existing tunnel, knowledge about the magnitude of vibration of the existing tunnel is of importance to avoid any damage in it, prior to the blasting operation. But the mounting of any vibration measuring devices is often prevented by the daily use of the tunnel, so that estimation must be done without direct measurement. Therefore, it is necessary that the dynamic behavior of the existing tunnel must be presumed by means of monitoring the vibration of the newly constructed tunnel.

The above mentioned results can be used for this estimation of the vibration of the existing tunnel. The results show that the magnitude of vibration in the existing tunnel is greater than that in the new one, even though the measuring points are at the same distance from the blast.

Fig. 3 showing the particle motion in both tunnels, indicates that the bottom of Tunnel A mainly vibrates in the vertical direction, but the bottom corner of Tunnel B seems to vibrate in a line through the centroid of the tunnel cross section. Therefore, it is noted that the vertical components of measurement are strongly influenced by the place where the measurements are done. If the measurements are taken at the center of the bottom, the magnitude would be greater than those obtained at a corner or side wall.

(2) Orientation of Energy Propagation from the Blast Zone

It has been seen from Fig. 2 that the greater magnitudes of particle velocity are measured in Tunnel A as the face of Tunnel B approaches the crossing point, compared with those obtained as the face leaves beyond the crossing. To show this more clearly, the measurements are continuously taken at Tunnel A for each blast progressing the face of the upper part of Tunnel B.

By assuming that the particle velocity is proportional to $W^{2/3}$ (W: charge weight), the particle velocity for a unit charge is expressed in Fig. 4 as a function of the location of the blast. It appears from the figure that the magnitude of particle velocity becomes a maximum when the face of Tunnel B arrives at a little before the crossing point, not exactly at the crossing where the distance between the measuring point and blast zone becomes the shortest.

It is also clear that there seems to be a non-uniformity in the orientation of the travelling wave, propagated from the blast zone. The energy is propagated mainly in the direction of tunnel progression, rather than in the backward direction. This non-uniformity may be due to the free boundary of the tunnel face.

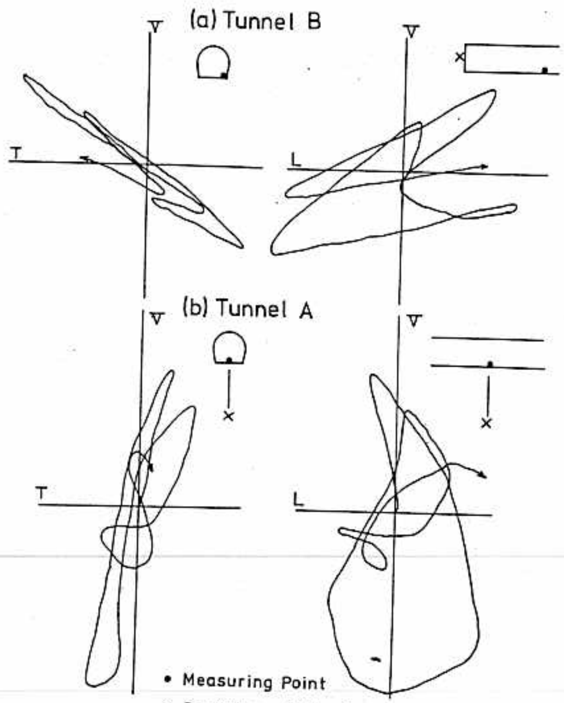

Fig. 3 Particle Motion

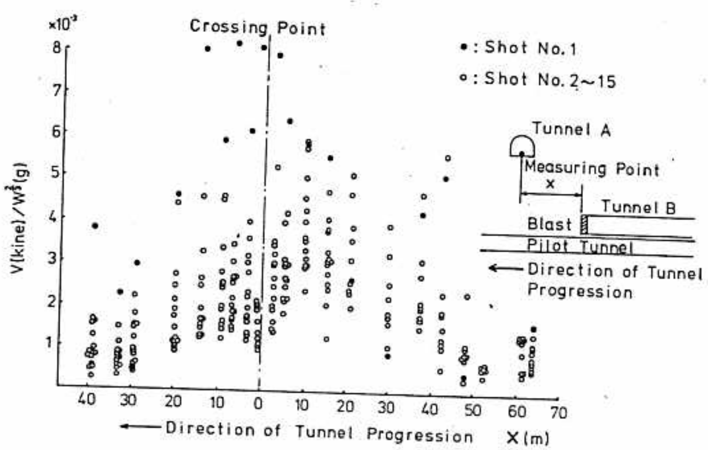

Fig. 4 Particle Velocity in Tunnel A due to Progression of Tunnel B

In Fig. 5, particle velocity magnitudes in both tunnels are plotted against the distances between the blast zone and the measuring points. It is obvious that the regression lines in these figures are quite different from each other. Vibration of Tunnel A decreases more rapidly with distance than Tunnel B. These differences come from the different wave paths from the blast zone. Assuming that there is similar geometrical relation between the case as shown in Fig. 5 (b) and the case where the tunnel face approaches a measuring point, as shown in Fig. 4, the following relation is valid among particle velocity ν (kine), charge weight W (gr) and distance r (m),

$$\nu = CW^{2/3}r^{-2.7} \tag{1}$$

where C is a constant, depending on the method of blasting, nature of rock and type of charge. It is seen that the constant C is a factor giving the magnitude of energy transmitted into the medium. The results calculated show that the constant C decreases as the blast zone approaches the measuring point. The results are plotted as a function of the angle between the tunnel axis and the direction to the measuring point, as shown in Fig. 6.

It may be concluded that the energy is not uniformly propagated in all directions, but much of the energy is transmitted in the direction of tunnel progression.

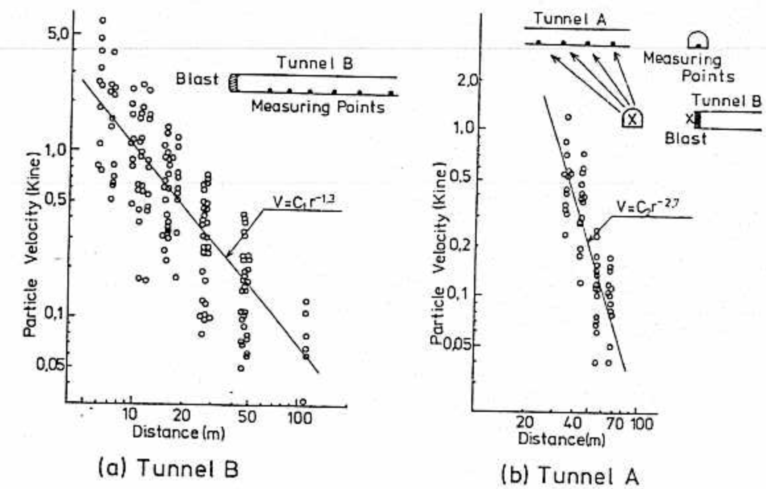

Fig. 5 Regression Lines of Particle Velocity (Vertical Component)

3. Effects of Blasting on Tunnel Lining

3.1 Test Sites

Field experiments have been conducted at two different sites having tunnels with concrete linings. One is a utility tunnel embedded beneath building land (called Site 1). The other is a bypass tunnel at a dam construction site (called Site 2). Configurations of the blast holes, charge weight as well as the geometrical relation of both tunnels are shown in Fig. 7 (a) and (b). The types of charge were dynamite and AN-FO. The charges were fired from a farther point, so as not to damage the ground through which wave travelled. Rocks around the tunnel are granite at Site 1 and liparite at Site 2. For both sites, there are no surface soil layers. The propagation velocities of the longitudinal wave at Site 1 and 2 are in the range of $2\sim3$km/s and $2.5\sim4.4$km/s, respectively.

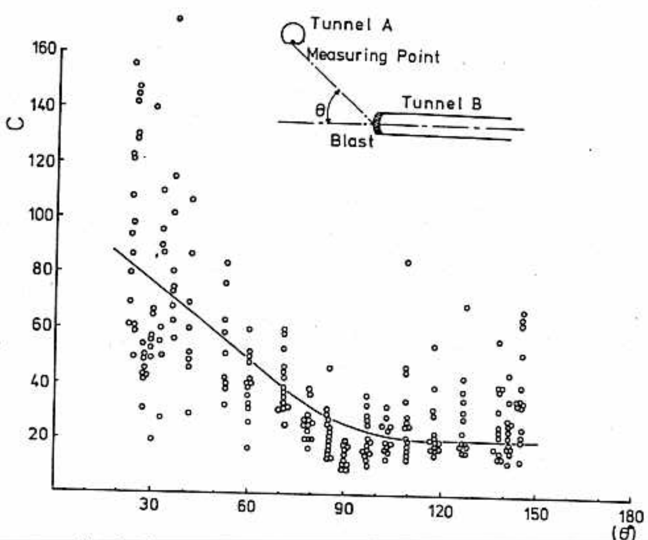

Fig. 6 Orientation of Energy Propagation from Blast Zone

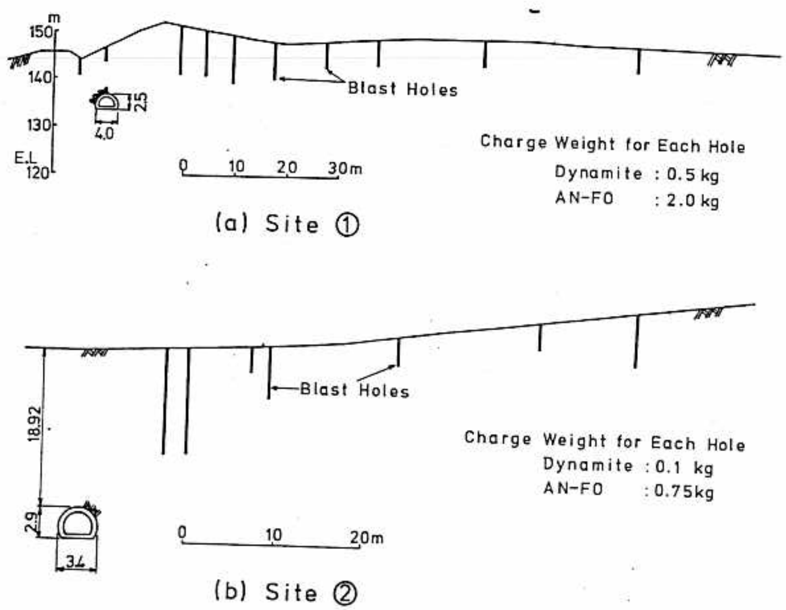

Fig. 7 Section View of Test Sites

3.2 Instrumentation

The measuring devices used in these field works were, electromagnetic-type velocity gages (Geo-space: natural frequency $f_0 = 4.5$Hz), mini-accelerometers (Kyowa: natural frequency $f_0 = 750$Hz, max. 50G) and SR-4 strain gages (G.L. = 67mm). These measuring devices were mounted on the internal surface of the concrete lining, and the gage arrays are shown in Fig. 8. The vertical and horizontal components of particle velocity and acceleration were measured. The horizontal components were all in a direction perpendicular to the tunnel axis. For strain, circumferential components along the internal surface of the lining were obtained, and the radial components within the lining were measured by molded SR-4 strain gages.

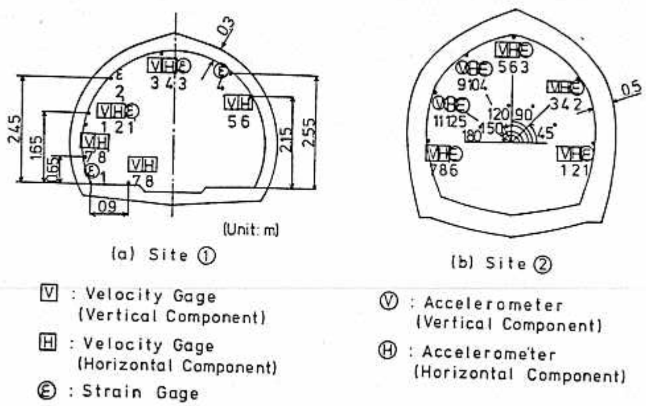

Fig. 8 Location of Measuring Points

3.3 Results and Discussions

(1) Seismogram of Particle Velocity and Propagation Equation

Some of the seismograms of particle velocity measured at the ground surface and on the internal surface of the lining, are shown in Fig. 9. The data for the lining are obtained at the measuring point facing the blast zone. It is obvious that particle velocity on the ground surface is strongly influenced by the free boundary of the ground. The data for both Site 1 and 2 are plotted in Fig. 10, to determine propagation equations relating the magnitude of peak particle velocity to distance. In these figures the magnitudes of the initial peak and the maximum after the initial are included only in the figure showing the ground surface measurement.

The empirical propagation equation may be written in the following general form,

$$v = CW^{\beta}r^{-\alpha} \tag{2}$$

where v is particle velocity, r is distance between blast zone and measuring point, W is charge weight, and C, β, α, are all positive coefficients.

It is noted that the regression lines shown in Fig. 10 are similar, so that the decay exponent α can be assumed to be $\alpha = 2$ for both cases of the ground surface and the lining, i.e. the magnitude of particle velocity decreases with square of the distance.

(2) Particle Velocity Distributions on Lining

Distributions of particle velocity on the lining for Sites 1 and 2 are shown in Fig. 11 and 12, respectively. Fig. 11 is the result of the blasting operation at a distance of 24m from the lining, and Fig. 12 is for 15m. These figures are obtained by plotting the particle velocity at each measuring point, as a vector, originating from the undeformed lining axis. It is obvious that the maximum particle velocity on the lining may occur at a point facing the blast zone or at its crown.

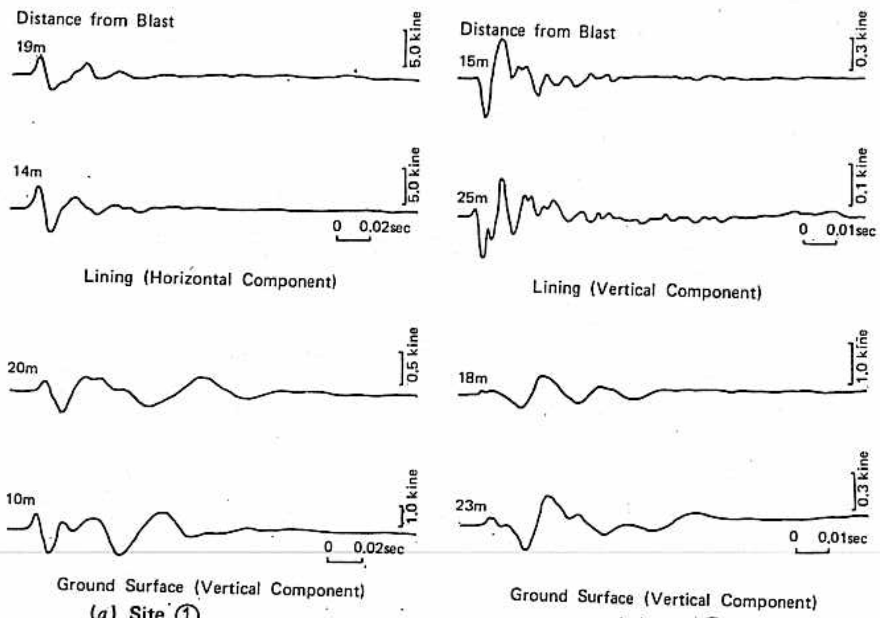

Fig. 9 Seismograms of Particle Velocity

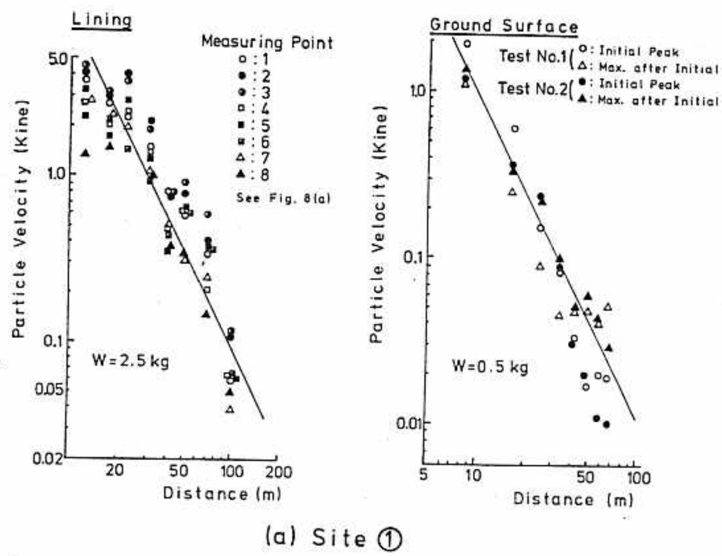

Fig. 10 (a) Regression Lines of Vertical Component of Particle Velocity

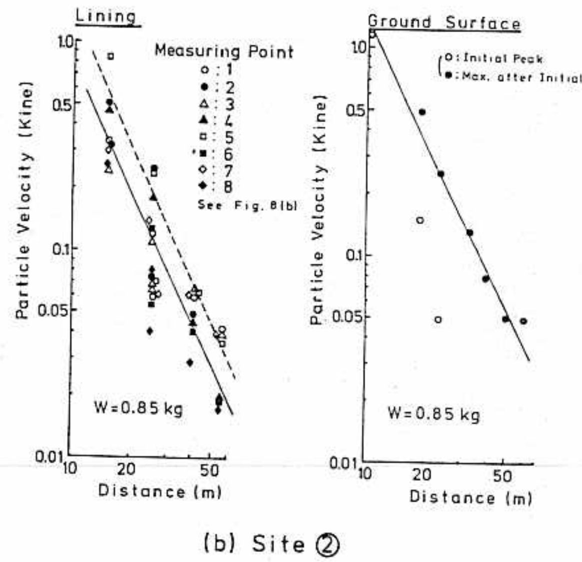

Fig. 10 (b) Regression Lines of Vertical Component of Particle Velocity

(3) Relation between Particle Velocity and Strain on Surface of Lining

Strain is not associated with rigid motion but particle velocity contains a component of rigid motion. The particle velocity essentially differs from the strain. Therefore, the maximum strain does not necessarily occur at the same place as where the particle velocity becomes a maximum. Some of the seismograms of circumferential strain on the surface of lining are shown in Fig. 13. The distributions of particle velocity and strain on the internal surface of the lining for Site 2 are given in Fig. 14.

It is obvious from the experimental results shown in Fig. 14 (a) that the radial component of particle velocity gives a maximum value at $\theta = 90^\circ$, i.e. at the arch crown. On the other hand, the maximum value of circumferential strain is obtained at roughly $\theta = 45^\circ$ or 150°. It is noted from these results that the point giving the maximum particle velocity does not coincide with one giving the maximum strain. This is also obvious from the theoretical results shown in Fig. 14 (b). These theoretical solutions are for the case of sinusoidal harmonic motion. But it has been verified that the difference between sinusoidal harmonic solution and one for a single sinusoidal pulse becomes negligibly small if the wave length is more than three times larger than tunnel diameter.[1)]

Experimental results for the radial component of particle velocity give the maximum value at the crown ($\theta = 90^\circ$), but they differ from the theoretical solutions in which the maximum value occurs at the point facing the blast zone ($\theta = 55^\circ$). This discrepancy may arise as follows; a) There usually exists an opening between the arch crown and the surrounding medium so that the radial particle velocity at the crown becomes extremely large. b) There is much loosening in the medium behind the arch crown.

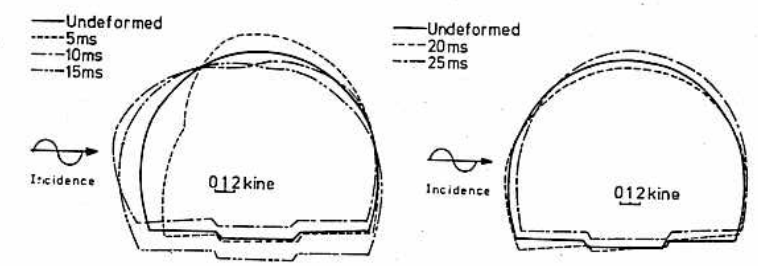

Fig. 11 Particle Velocity Distributions in Concrete Lining (Site (1))

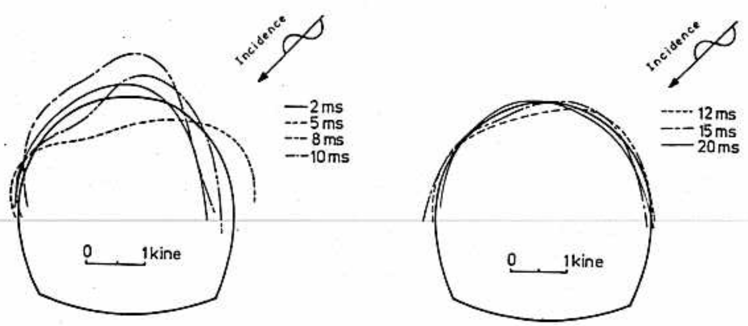

Fig. 12 Particle Velocity Distributions in Concrete Lining (Site (2))

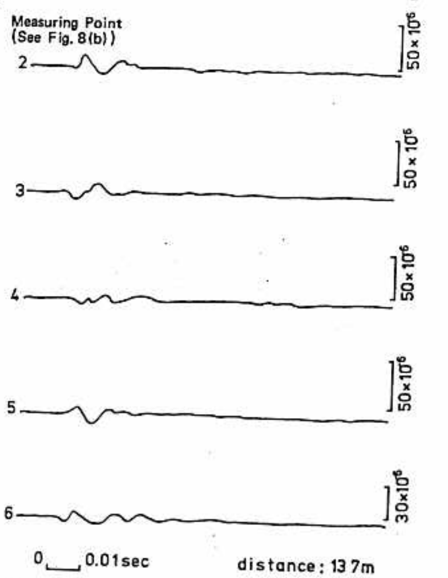

Fig. 13 Seismogram of Circumferential Strain (Site (2))

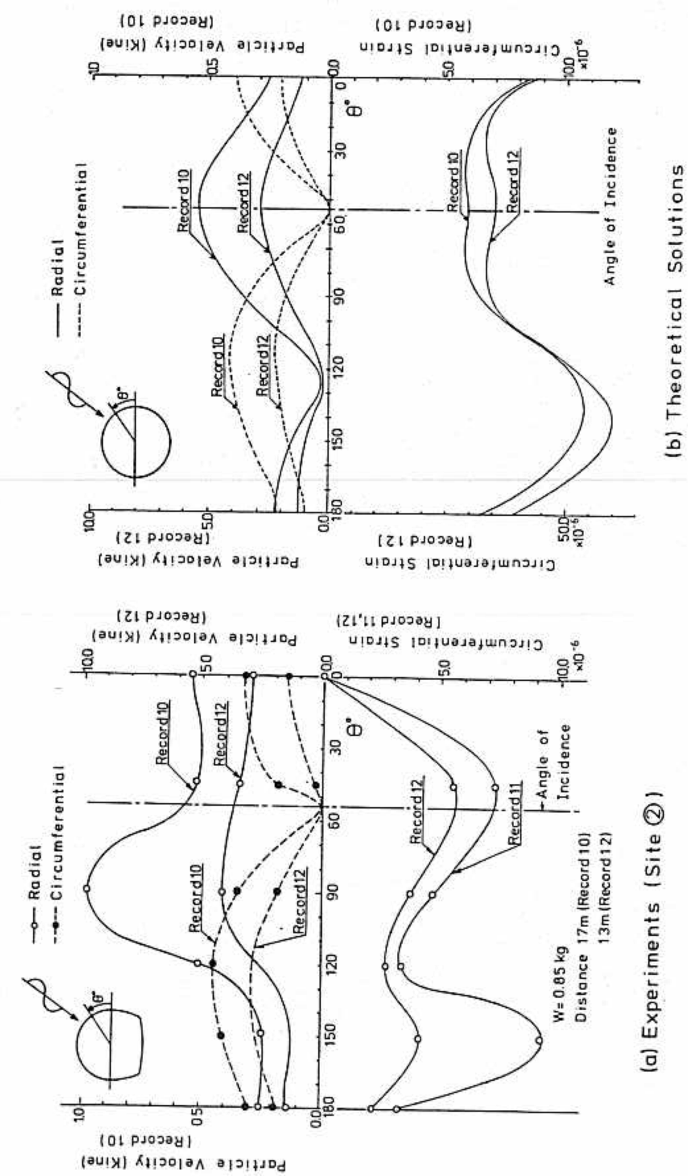

Fig. 14 Distribution of Particle Velocity and Strain

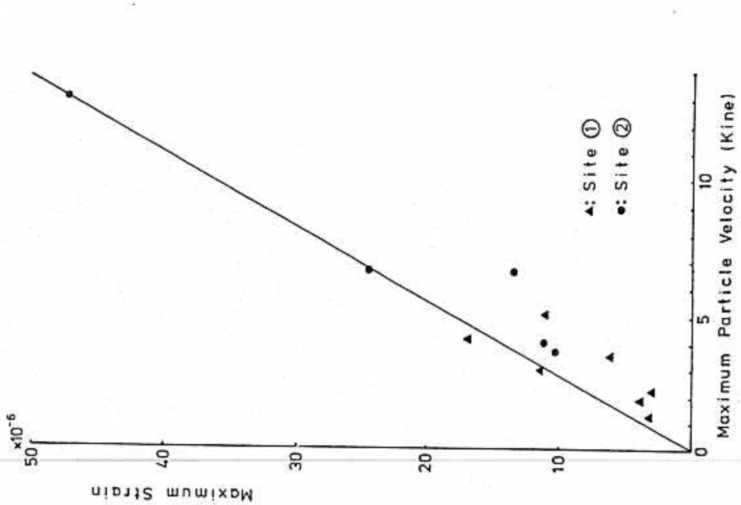

Fig. 16 Relation between Maximum Particle Velocity and Maximum Strain on Tunnel Lining

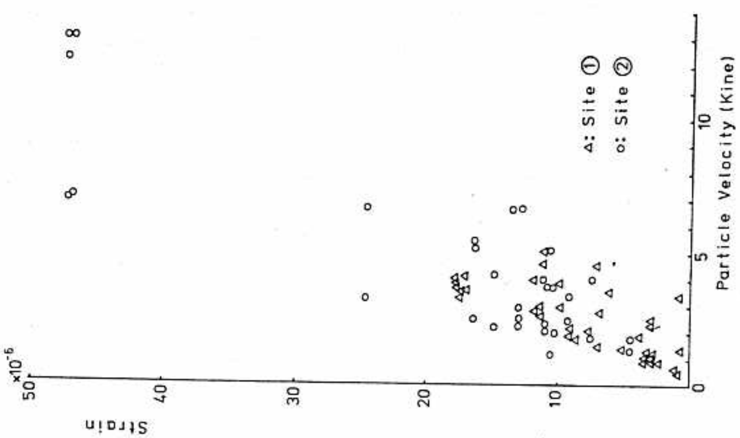

Fig. 15 Relation between Particle Velocity and Strain on Tunnel Lining

Fig. 15 shows the relation between particle velocity and strain, both of which are obtained at the same time and at the same measuring point. From this figure, it is clear that the strain cannot uniquely be determined by particle velocity because of their different distributions along the lining. Plotting the maximum particle velocity against the maximum strain, even though they occur at the different points, gives Fig. 16, which shows a linear relation between those two magnitudes. The place where the measurements are obtained is of fundamental importance in discussing the relation between strain and particle velocity.

The strain ε is often estimated through particle velocity ν by the following equation:

$$\varepsilon \doteqdot \nu / C \tag{3}$$

where C is usually chosen to be constant. But, according to the theoretical solution, the constant depends on the geometrical relation of the tunnel, relative rigidity of lining and medium, and frequency of vibration, as shown in the following form.

$$\frac{1}{C} = \frac{G_1 k_1'^2 \,|\, S(r) \,|}{2\pi f k_1 \,|\, H_1^{(2)}(k_1 r) \,|} \cdot \frac{\sigma^*}{E_2 \nu^*} \tag{4}$$

where, $S(r) = H_2^{(2)}(k_1 r)/\kappa^2 + H_0^{(2)}(k_1 r)\cdot(1/\kappa^2 - 1)$

$\kappa = \sqrt{2(1-\nu)/(1-2\nu)}$

ν : Poisson's ratio of medium

k_1 : $2\pi f / V_p$

f : Frequency

V_p : Propagation velocity of longitudinal wave

$k_1' = \kappa \cdot k_1$

G_1 : Shear modulus of medium

E_2 : Young's modulus of lining

σ^* : Concentration factor of stress

ν^* : Concentration factor of particle velocity

$H_n^{(2)}$: Nth order Hankel function of 2nd kind

r : Distance from blast zone

The linear relation between the maximum particle velocity and the maximum strain, shown in Fig. 16, gives that the particle velocity for failure of the lining becomes approximately 35 kine (cm/s) on an assumption that tensile stress for failure of concrete is 20kg/cm². In fact, it has been reported that crack initiation occurred on a concrete tunnel lining at the particle velocity of 33.8 kine.[2)]

(4) Radial Strain Within Lining

The strain discussed in the previous section was that on the surface of lining. The next question is what about strain within the lining. A result of the measurement is shown in Table 1, which shows the magnitude of the initial peak when the wave arrives at the lining. These data are those for the measuring point facing the blast zone.

Table 1 Strains within Lining

	Tangential component on the surface		Radial component within lining			
Distance from internal surface (cm)	0.0*	0.0**	2.5	17.5	32.5	45.5
Strain (x10⁻⁶)	38.2	32.8	-17.0	-9.4	-1.9	0.0

* Tunnel axis direction
** Circumferential direction

(- : Compression, + : Tension)

It is noted from the result that the radial strains within the lining are all compressive for the initial peak, and their magnitudes increase at measuring points near to the internal free surface of the lining. On the other hand, strains at the surface of the lining are tensile, the magnitudes of which are larger than those of compression within the lining. It is concluded, therefore, that the maximum tensile strain occurs at the surface.

4. Conclusions

The results obtained herein are summarized as follows:

(1) Even though the distances from the blast zone are the same, a large vibration may occur in an existing tunnel (Tunnel A), rather than in a newly constructed tunnel (Tunnel B) where the blasting operation is conducted. Therefore, if the measurements obtained in Tunnel B are used for estimating the vibration of Tunnel A, care in estimation is necessary, because it is not on the safe side.

(2) When the face of Tunnel B approaches Tunnel A, blast control is of much importance, so as not to damage Tunnel A, in comparison with when the face passes through or leaves the crossing point.

(3) The slopes of regression lines for particle velocity versus distance are approximately the same for both measurements obtained on the surface of the concrete tunnel lining and on the ground surface.

(4) The vertical component of particle velocity at the arch crown of the lining gives the maximum value. This may be due to an opening or loosening of medium behind the arch crown. Apart from the arch crown, the particle velocity in any position facing the blast zone is also remarkably high.

(5) The place where the maximum strain occurs is not necessarily the same as where the particle velocity gives the maximum value.

(6) The maximum strain seems to be proportional to the maximum particle velocity, and its proportionality constant may be a function of the geometrical relation, relative rigidity of lining and ground medium, and frequency, even though they occur at different places on the lining.

(7) The radial strain within the lining facing the blast zone is compressive at the initial peak and its magnitude is always small, compared with the tensile strain obtained at the surface of the lining.

5. Acknowledgments

The authors acknowledge Kobe and Takarazuka Municipal Offices for their financial support for this study. The authors also wish to express their sincere thanks to Mr. K. Miyagawa, Mr. K. Yoshida and Mr. I. Kitada for analyzing the field data. Special thanks are also due to Mr. S. Kasai for solving the analytical problems.

References

(1) Y. Niwa, S. Kobayashi and T. Matsumoto; Transient Stresses Produced around Tunnels by Traveling Waves, Journal of the Society on Materials Science, Japan Vol. 23, No. 248, 1974, pp. 361 ~ 367.

(2) H. Okazawa, et al.; The Effect of Vibration in Nearby Tunnels Caused by Blasting and Its Preventive Measures – The Case of Koi-Tunnel on Sanyo-Shinkansen, Tunnels and Underground, Vol. 6, No. 11, 1975, pp. 789 ~ 797.

(3) S. Kasai; Theoretical Study on Dynamic Behaviors of Tunnel Lining, M.S. Thesis, Kobe University, 1974.

STUDY OF UNDERGROUND STRUCTURAL STABILITY USING NEAR-SURFACE AND DOWN-HOLE MICROSEISMIC TECHNIQUES

H. Reginald Hardy, Jr.[1] and Gary L. Mowrey[2]

1. Introduction

When stressed, most solids emit bursts of microlevel acoustic energy. This phenomenon is commonly termed microseismic activity, although synonymous terms such as acoustic emission, rock noise, and seismo-acoustic activity are often utilized. In geologic materials, relatively little is known in regard to the basic mechanisms responsible for microseismic activity. Such activity, however, is known to be associated with mechanical instability within the material; and with suitable instrumentation, it is possible to locate the source of the instability and to evaluate its intensity. Microseismic activity therefore, provides the research worker and the engineer with an indirect means of monitoring the internal stability of a field structure, and as such, forms the basis for one of the most useful tools presently available in rock mechanics.

In recent years extensive use has been made of microseismic techniques for evaluating the stability of such geologic structures as mines, rock and soil slopes, tunnels, earth filled dams, and more recently underground storage facilities. A more detailed discussion of the microseismic concept and details of a variety of applications is available in a number of recent publications [for example, Hardy (1971, 1972, 1973, 1975) and Hardy and Leighton (1977)].

Microseismic activity at a field site is monitored by installing a suitable transducer, or usually a number of transducers (an array), in locations where they can detect any microseismic activity which may be

[1]Chairman Geomechanics Section, and Director, Rock Mechanics Laboratory, Department of Mineral Engineering, College of Earth and Mineral Sciences, The Pennsylvania State University, University Park, Pennsylvania, U.S.A.

[2]Research Assistant, Geomechanics Section, Department of Mineral Engineering, College of Earth and Mineral Sciences, The Pennsylvania State University, University Park, Pennsylvania, U.S.A.